J Neurophysiol 115: 2389–2398, 2016.
First published February 24, 2016; doi:10.1152/jn.00652.2015.

Encoding of natural sounds by variance of the cortical local field potential

Nai Ding,[1] Jonathan Z. Simon,[2,3,4] Shihab A. Shamma,[2,4] and Stephen V. David[5]

[1]*College of Biomedical Engineering and Instrument Sciences, Zhejiang University, Zhejiang, China;* [2]*Department of Electrical and Computer Engineering, University of Maryland, College Park, Maryland;* [3]*Department of Biology, University of Maryland, College Park, Maryland;* [4]*Institute for Systems Research, University of Maryland, College Park, Maryland; and* [5]*Oregon Hearing Research Center, Oregon Health and Science University, Portland, Oregon*

Submitted 30 June 2015; accepted in final form 17 February 2016

Ding N, Simon JZ, Shamma SA, David SV. Encoding of natural sounds by variance of the cortical local field potential. *J Neurophysiol* 115: 2389–2398, 2016. First published February 24, 2016; doi:10.1152/jn.00652.2015.—Neural encoding of sensory stimuli is typically studied by averaging neural signals across repetitions of the same stimulus. However, recent work has suggested that the variance of neural activity across repeated trials can also depend on sensory inputs. Here we characterize how intertrial variance of the local field potential (LFP) in primary auditory cortex of awake ferrets is affected by continuous natural sound stimuli. We find that natural sounds often suppress the intertrial variance of low-frequency LFP (<16 Hz). However, the amount of the variance reduction is not significantly correlated with the amplitude of the mean response at the same recording site. Moreover, the variance changes occur with longer latency than the mean response. Although the dynamics of the mean response and intertrial variance differ, spectro-temporal receptive field analysis reveals that changes in LFP variance have frequency tuning similar to multiunit activity at the same recording site, suggesting a local origin for changes in LFP variance. In summary, the spectral tuning of LFP intertrial variance and the absence of a correlation with the amplitude of the mean evoked LFP suggest substantial heterogeneity in the interaction between spontaneous and stimulus-driven activity across local neural populations in auditory cortex.

auditory cortex; local field potential; response variance; spectro-temporal receptive field; speech

LARGE-SCALE NEURAL ACTIVITY, measured by the local field potential (LFP), electroencephalography (EEG), or magnetoencephalography (MEG), has been extensively studied in humans and other mammals to characterize network-level neural dynamics involved in sensory processing (Lakatos et al. 2005; Steinschneider et al. 2008; Szymanski et al. 2011). Since these large-scale neural signals can be measured both by implanted microelectrodes and noninvasively by EEG or MEG, they provide a critical bridge between single-unit animal neurophysiology and noninvasive human neurophysiology. During the presentation of complex sounds, extracranially measured EEG and MEG responses and intracranially measured LFP signals are phase locked to the slow temporal modulations of sounds (i.e., the sound envelope). Sound envelope-locked signals have been reported across a large number of cortical areas, including primary auditory cortex (A1) (e.g., Eggermont 2002) and sensory areas not specifically involved in auditory processing (e.g., Lakatos et al. 2008).

Traditionally, sensory coding by the LFP is characterized by its mean response, i.e., activity averaged across multiple repetitions of the same stimulus (Eggermont et al. 2011). The mean response mainly reflects stimulus-locked neural activity. Recently, however, it has been suggested that sensory stimuli change not just the mean response but also the variance of neural activity over trials, here termed intertrial variance (Churchland et al. 2010; Crone et al. 2001). The intertrial variance mainly reflects the power of non-stimulus-locked neural activity. Single-unit spiking activity can generally by described by Poisson statistics, where the intertrial variance scales proportionately with the mean responses. However, for LFP the interaction between mean response and intertrial variance can take several different forms, depending on both single-neuron activity and synchrony of neurons across the neural network (Ecker and Tolias 2014; Goris et al. 2014; Lin et al. 2015; Telenczuk et al. 2010). In one extreme case, stimulus-locked neural responses are generated by resetting the phase of spontaneous neural oscillations. In other words, spontaneous activity is converted into stimulus-driven activity and therefore the variance of neural activity, reflecting the power of non-stimulus-locked neural activity, will be reduced by sensory stimuli (Fig. 1*A*) (Hanslmayr et al. 2007; Kayser et al. 2009; Lakatos et al. 2009; Luo and Poeppel 2007; Makeig et al. 2002). In another extreme, if precisely stimulus-locked neural responses are generated independent of spontaneous neural activity, the intertrial variance of measured neural responses reflects the power of spontaneous neural activity and should be invariant to sensory stimuli (Fig. 1*B*) (Ding and Simon 2013; Howard and Poeppel 2010, 2012; Makinen et al. 2005; Shah et al. 2004; Yeung et al. 2004). If neural responses are loosely phase locked to the stimulus and are independent of spontaneous neural activity, the intertrial variance of neural activity will be increased (Fig. 1*C*) (Krause and Banks 2013; Truccolo et al. 2002). Finally, even if a sensory stimulus does not generate any phase-locked response, it can suppress spontaneous neural activity (Fig. 1*D*) (Churchland et al. 2010), not affect neural activity at all (Fig. 1*E*), or generate an increase in non-stimulus-locked neural activity (Fig. 1*F*) (Crone et al. 2001).

Questions about intertrial variance have contributed to an ongoing controversy in sensory neuroscience: whether stimulus-stimulus-locked LFP/EEG/MEG responses are generated by resetting the phase of ongoing neural oscillations, i.e., the phase resetting theory shown by Fig. 1*A*, or by an additive response component independent of ongoing activity, i.e., the additive response theory shown by Fig. 1, *B* and *C*. The phase resetting theory predicts that intertrial variance should decrease, while the additive response theory does not generate any specific prediction about intertrial variance. For recordings from different cortical areas and under different behavioral

Address for reprint requests and other correspondence: N. Ding, College of Biomedical Engineering and Instrument Sciences, Zhejiang Univ., Zhejiang, China 310027 (e-mail: ding_nai@zju.edu.cn).

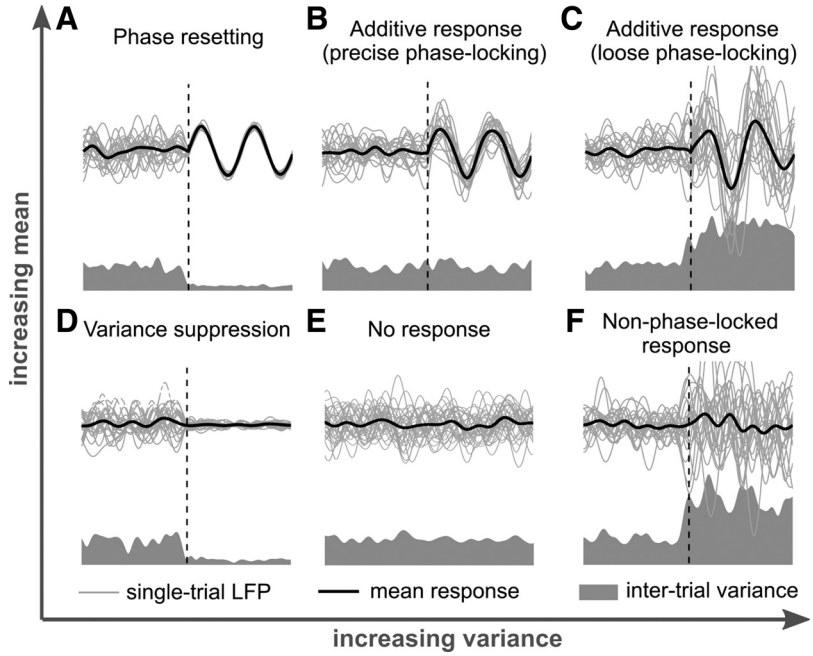

Fig. 1. Schematic illustrations of how the mean and variance of neural signals may be affected by a sensory stimulus. In all panels, the gray curves at *top* are 20 simulated single-trial LFP waveforms aligned to stimulus onset (vertical line). The black curve shows the average over 20 trials, and shaded areas at *bottom* show the intertrial variance. *A*: if the response reflects phase resetting of spontaneous activity, the mean stimulus-evoked response is accompanied by a decrease in response variance. *B*: if the response is perfectly phase locked (i.e., synchronized) to the stimulus but independent of spontaneous neural activity, response variance is not affected by the stimulus. *C*: if the stimulus-aligned response is independent of spontaneous neural activity but has imprecise phase locking, the response variance is increased by the stimulus. *D*: if the stimulus suppresses spontaneous neural activity without producing a phase-locked response, then a decrease in variance will also be observed. *E*: if the stimulus evokes no response, then no change will be observed in the mean response or response variance. *F*: finally, if the stimulus generates a non-phase-locked response, independent of spontaneous activity, then an increase in response variance will be observed.

states, the intertrial variance of low-frequency LFP has been reported to increase (Krause and Banks 2013; Truccolo et al. 2002), decrease (Churchland et al. 2010), or remain unaffected (Makinen et al. 2005) by sensory stimuli. Therefore, there is no consistent answer about whether sensory stimuli increase or decrease response variance, and it remains unclear whether this heterogeneity is due to differences in cortical areas or whether it even exists among neural populations within the same cortical area. Furthermore, properties of the intertrial variance vary across LFP frequency bands (Steinschneider et al. 2008) and also between stimulus onset and periods of sustained stimulation (Fuentemilla et al. 2006). In sum, intertrial variance may depend on behavioral state, cortical area, the local neural population within an area, the frequency band of LFP activity, and the duration of sensory stimulation. This study controls the behavioral state (i.e., passive listening) and the recording area (i.e., auditory cortex) and investigates how the intertrial variance is affected by sound stimuli over time, LFP band, and local neural populations.

Here we ask specifically how the presentation of a natural sound affects intertrial variance across LFP frequency bands in A1 and whether the intertrial variance of LFP is tuned to spectro-temporal sound features. Data were collected from the awake passive-listening ferret, a carnivore whose auditory cortex shares basic anatomical and functional properties with that of many other mammals (Hackett 2011). Sensory activity was measured using continuous human speech, a complex natural sound with spectro-temporal properties comparable to other mammalian vocalizations (Lewicki 2002; Singh and Theunissen 2003) and one that allows for comparison to noninvasive studies of representation of speech in humans.

METHODS

Experimental procedures. Extracellular neural activity was recorded from A1 of 11 awake, passively listening ferrets. Data were acquired from 477 recording sites in both hemispheres. All experimental procedures conformed to standards specified by the National Institutes of Health and were reviewed and approved by the University of Maryland Animal Care and Use Committee. Surgical preparation procedures are described in David et al. (2009). Recordings were made with tungsten microelectrodes (1–5 MΩ; FHC) in awake, head-fixed animals in a double-walled, sound-attenuating chamber (Industrial Acoustics). During each recording session, one to four electrodes were positioned by independent microdrives and neurophysiological activity was recorded with a commercial data acquisition system (Alpha-Omega). Line noise was removed online by a 60-Hz notch filter. Analysis of some single-unit data collected during these experiments has been published previously (David et al. 2009).

Stimuli. Thirty sentences from the TIMIT database (Garofolo 1993), spoken by 30 different speakers, were employed as the stimuli. Each 3-s sentence was presented at 65 dB sound pressure level (SPL) for 2–8 repetitions (5.2 repetitions on average) in random order on each repetition. The recordings contained pre- and poststimulus silent periods of 400 ms for 309 sites and irregular pre- and poststimulus periods (0–1,200 ms) for the remaining 168 sites. Only the subset of recording sites with 400-ms pre- and poststimulus silent periods were included in the comparison of stimulus-driven and baseline, spontaneous activity (e.g., Fig. 2 and Fig. 3).

Filtering of neurophysiological signals. The LFP was obtained by low-pass filtering the raw extracellular recording below 600 Hz, and multiunit activity (MUA) was measured as the time-varying power of the neural recording after band-pass filtering between 600 and 3,000 Hz. The LFP was further filtered into different frequency bands, roughly corresponding to those commonly defined for EEG and LFP recordings (delta: 2–4 Hz, theta: 4–8 Hz, alpha: 8–16 Hz, beta: 16–32 Hz, gamma: 32–64 Hz, high gamma: 64–160 Hz). This processing used FIR filters based on a 267-ms Hamming window. The time delay produced by the linear-phase FIR filter was compensated by shifting the filtered signal 133 ms back in time.

Mean and variance of neural responses. The time-varying LFP response to a stimulus can be decomposed into two components. One is the mean response across trials, the component reliably phase locked to the stimulus across trials. The mean response is sometimes referred to as the evoked response (Tallon-Baudry and Bertrand 1999). The second component is the difference between single-trial responses and the mean response, which characterizes neural activity that is not phase locked with the stimulus and is sometimes referred to as the induced response (Tallon-Baudry and Bertrand 1999). This

component is measured by the variance of the LFP over trials, or intertrial variance.

The decomposition of LFP into mean response and intertrial variance is expressed mathematically as follows. Suppose the time-varying neural response in the kth trial is $x_k(t)$, for K total trials. In the following, the time variable, t, is omitted for compactness. Each single-trial response is decomposed into the mean response, i.e., $v = (\sum_k x_k)/K$, and a non-stimulus-locked remaining component, i.e., $x_k - v$. The power of the non-stimulus-locked response, $x_k - v$, is $P_I = \sum_k (x_k - v)^2/K$, the same as the variance of the response over trials. Furthermore,

$$P_I = \left(\sum_k x_k^2\right)/K - v^2$$

The first term on the right-hand side, $(\sum_k X_k^2)/K$, is the mean power of single-trial LFP, referred to here as the total power P_T. The second term, v^2, is the power of the mean response P_M. Therefore, $P_T = P_I + P_M$, and the total power is the linear sum of the power of the stimulus-locked component and the power of the non-stimulus-locked component.

This study primarily addresses how LFP power, including contributions from both the stimulus-locked and the non-stimulus-locked components, is changed by the presentation of an auditory stimulus. For both the power of the mean response and the intertrial variance, the stimulus-related change in power is defined as the decibel difference between the response power during stimulus presentation and during the prestimulus period. In the prestimulus period, there is no stimulus-related activity and therefore no stimulus-locked LFP response. Thus during this period the mean response averaged over trials reflects spontaneous activity only, and $P_M = P_T/K$.

In this study, each stimulus was repeated only a few times (5.2, on average), which typically creates difficulty in reliably estimating the mean and intertrial variance of the neural response to a single stimulus. However, this difficulty was alleviated by the fact that there were 30 distinct 3-s stimuli in the data set. To achieve reliable estimates, stimulus-related changes in mean and intertrial variance were first calculated separately for each stimulus and then averaged over all stimuli. For some analyses, they were also averaged over time.

Spectro-temporal receptive field estimation and analysis. Spectro-temporal receptive field (STRF) analysis was employed to model the encoding of spectro-temporal sound features by the intertrial variance of different LFP bands. The STRF was estimated using boosting with 10-fold cross-validation (David et al. 2007), based on the neural response and stimulus spectrogram. Details of the estimation procedure are described in Ding and Simon (2012b). The spectrogram of the stimulus contained 24 logarithmically spaced frequency bins spanning 180-8,000 Hz, and STRF time lags between the stimulus and response ranged from −20 to 130 ms. We focus on neural encoding of slow temporal modulations below 50 Hz, and therefore the neural signal and the stimulus spectrogram are both resampled to 100 Hz (David et al. 2009). To remove the influence of transient onset responses and focus on the spectro-temporal tuning of sustained neural responses, we excluded data from the first 500 ms of sound stimulation on each trial for the STRF analysis.

The same boosting algorithm was used to estimate STRFs for MUA and the LFP mean response. The predictive power of the STRF is defined as the correlation coefficient (Pearson's r) between the measured neural response and the predicted response [i.e., the convolution between the STRF and the stimulus spectrogram (David et al. 2009)]. Significant predictive power was evaluated by a permutation test. Chance-level predictive power was calculated by randomly shuffling the predicted response in time and computing the correlation coefficient between the actual response and the shuffled prediction. Repeating this procedure for 1,000 shuffles produced a distribution of correlation coefficients. The position of the actual prediction correlation in this distribution was used to directly measure the probability (i.e., P value) that the actual prediction correlation was produced by chance. For the STRF analysis, response variance was calculated based on the LFP signal in different frequency bands while the mean LFP response was not filtered into narrow frequency bands. The mean LFP was not broken down into frequency bands because a single linear STRF model simultaneously characterizes neural tracking in all modulation frequency bands. The STRF for mean activity in a single band can be obtained by filtering the STRF estimated from the broadband LFP mean response. In contrast, the STRF for the variance of a single band cannot be obtained by filtering the STRF for the variance of broadband LFP. Computing variance is a nonlinear operation, and therefore STRFs must be estimated separately for each band.

Since delta- and theta-band LFP have intrinsically slow temporal dynamics, we also tested whether extending the maximal time lag to 280 ms improved STRF performance for response variance in those frequency bands or for the mean LFP response. The STRFs with a longer time lag range were significantly better at describing the mean response (i.e., higher predictive power, 7% increase, $P < 10^{-10}$, paired t-test) but not significantly better at describing the response variance (<1% increase in predictive power, $P > 0.47$ for both bands). Therefore, we only report STRFs with the longer time lag range for the mean response.

To calculate the similarity between two STRFs, each two-dimensional STRF was reshaped into a one-dimensional vector, and the correlation coefficient was calculated between the two resulting vectors. To calculate the best frequency (BF), the absolute value of the STRF was summed over time, resulting in a frequency tuning curve. The BF was determined by the peak of this tuning curve. The bandwidth of the STRF was also determined from the frequency tuning curve as the number of bins with amplitude higher than half of the maximal amplitude at BF. To calculate the peak latency of an STRF, the absolute value of the STRF was summed over frequency, resulting in a temporal response function. Latency was determined by the peak of this temporal response function.

RESULTS

Sensory stimuli determine both mean and variance of LFP activity in auditory cortex. Neurophysiological recordings were obtained from 477 sites in A1 of ferrets passively listening to 30 sentences uttered by different human speakers. We investigated how the mean and variance of LFP across trials were affected by the stimulus presentation (illustrated in Fig. 1). Three aspects of the LFP activity were characterized. The power of the mean response reflects the strength of the stimulus-locked LFP response. The intertrial response variance is a complementary signal that characterizes the power of neural activity not phase locked to the stimulus. The third measure, i.e., the total power, is the average of the LFP power in single trials. Total power includes both the stimulus-locked LFP components and the non-stimulus-locked LFP components (see METHODS).

To study these effects in auditory cortex, we filtered the LFP into standard frequency bands (delta: 2–4 Hz, theta: 4–8 Hz, alpha: 8–16 Hz, beta: 16–32 Hz, gamma: 32–64 Hz, high gamma: 64–160 Hz) and measured the time course of changes in mean response and variance in each band during presentation of the speech stimulus (Fig. 2). The alpha-band LFP is used as an example to illustrate the analytical approach (Fig. 2*A*). The power of the mean response and the intertrial variance of alpha-band LFP were calculated across repetitions of each sentence and then averaged over different sentences. Averaging over sentences reduces modulations by specific spectro-temporal stimulus features but preserves the changes associ-

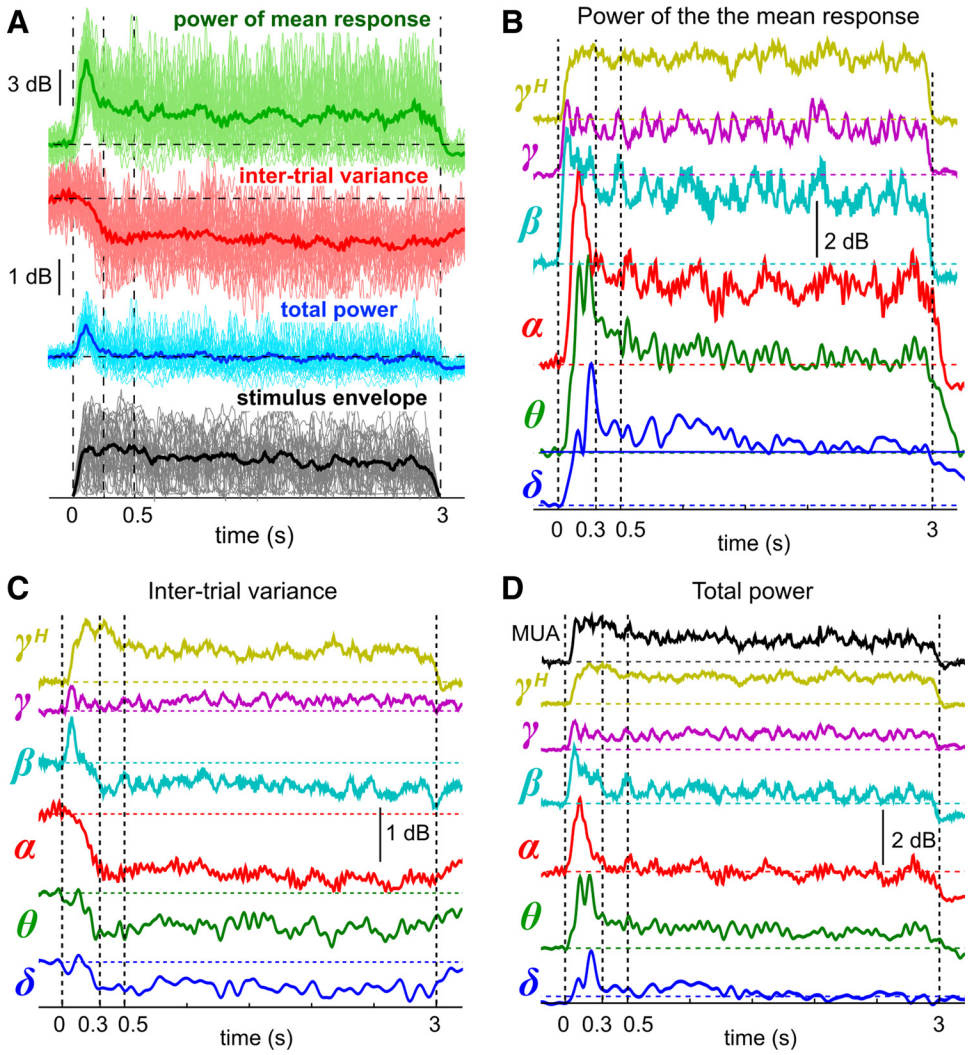

Fig. 2. Time course of the power of the response averaged over trials, intertrial variance, and total power. *A*: time course of the alpha-band LFP intertrial variance and the power of the mean response, averaged over all recording sites. The speech stimulus is presented from 0 to 3 s. Responses to individual sentences are indicated by the thin curves, and the average across all sentences is shown by the thick curves. Averaging over sentences smears out temporal fluctuations specific to individual sentences and emphasizes differences in power before, during, and after auditory stimulation. The mean response is increased by the stimulus, and intertrial variance is decreased (cf. Fig. 1*A*), but the latter occurs with a slower time course. The mean response shows a fast transient response, peaking at ~100 ms, while the intertrial variance gradually decreases over ~300 ms before reaching a steady state. *B–D*: time course of mean response, intertrial variance, and total power for each LFP frequency band, averaged over recording sites and stimuli. Mean response is increased in all frequency bands, while intertrial variance is decreased in the lower frequency bands (<32 Hz) and increased in the higher frequency bands (>64 Hz). γ^H, high gamma.

ated with the onset, duration, and offset of the speech stimuli. The power of the mean response in the alpha band shows a transient response, peaking at ~100 ms after the stimulus onset and followed by a sustained increase. The response variance, however, gradually decreases within the first ~300 ms after the stimulus onset and then remains suppressed throughout the period of stimulation (cf. Fig. 1*A*).

Figure 2, *B–D*, show the time course of the power of the mean response, intertrial variance, and total power for each LFP band, averaged over all recording sites. As expected from previous studies (Eggermont 2002), the mean response shows a sustained power increase in all LFP frequency bands during auditory stimulation. In low frequency bands (delta-beta) the mean response also shows a sharp transient power increase after stimulus onset. For intertrial variance, the effects of auditory stimulation are more variable across LFP bands. Variance gradually decreases in the delta, theta, and alpha bands (<16 Hz) after stimulus onset, while it gradually increases in the high gamma band (> 64 Hz). In the beta band, there is a transient increase in variance within the first 100 ms, followed by a sustained decrease. The total power of LFP shows a transient increase after stimulus onset in the delta, theta, alpha, and beta bands (<32 Hz) and a gradual increase in the gamma and high gamma bands (>32 Hz).

Figure 3 summarizes changes in response variance and power immediately following stimulus onset (Fig. 3*A*) and during sustained stimulation (Fig. 3*B*). The onset response is averaged over the first 300 ms after the stimulus onset, while the sustained response is averaged from 300 ms after the stimulus onset until the stimulus offset. In the low frequency bands (<16 Hz), the onset response is dominated by an increase in the mean response, leading the total power to also increase (cf. Fig. 1*B*), while the sustained response shows a roughly balanced increase in the mean response and decrease in intertrial variance (cf. Fig. 1*A*). Fig. 3, *C* and *D*, show the correlation between the stimulus-related changes in intertrial variance and mean response across recording sites. Changes in these two signals are not significantly correlated in the theta and alpha bands. However, the decrease in low-frequency LFP variance is correlated with the increase in high gamma power (Fig. 3*D*). In the gamma band, intertrial variance is barely affected by the stimulus for both the onset and the sustained responses, but the power increase in mean response leads the total power to increase in >75% of the recording sites (cf. Fig. 1*B*). In the high gamma band, increases in intertrial variance and mean response are strongly correlated.

Since the frequency bands below 16 Hz all showed sustained power increase in mean response and sustained decrease in

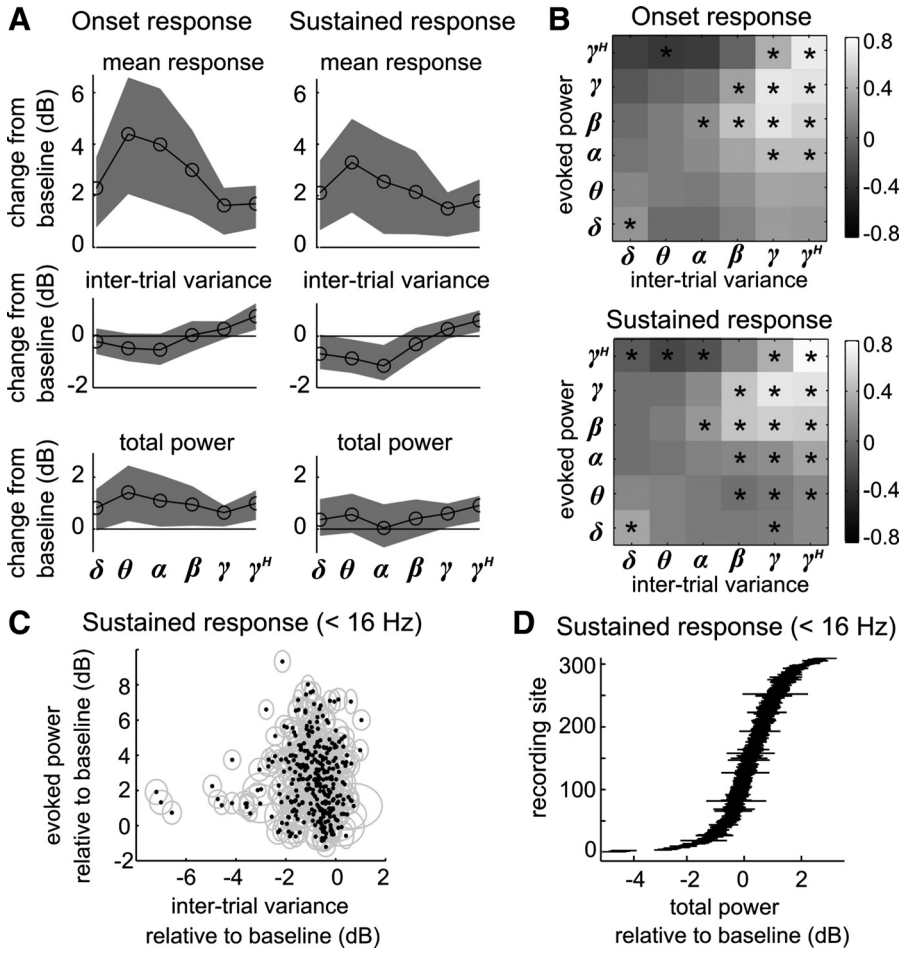

Fig. 3. Average stimulus-related changes in intertrial variance, power of the mean response, and total power across LFP bands. *A*: changes in each band immediately following stimulus onset (0–0.3 s) or during sustained auditory stimulation (0.3–3 s), plotted relative to the baseline prestimulus period. The onset response is dominated by an increase in mean response, leading to an increase in total power. For the sustained response, lower frequency bands (delta, theta, and alpha) show a roughly balanced increase in mean response and decrease in response variance, while the high gamma band shows an increase in both mean response and response variance. The area between the 25th and 75th percentiles of individual recording sites is shaded. *B*: correlation between stimulus-related changes in intertrial variance and mean response across recording sites following stimulus onset or during sustained auditory stimulation. Similar patterns are observed for the onset response and the sustained response. In theta and alpha bands, changes in mean response and intertrial variance are not significantly correlated. However, changes in mean response and intertrial variance in the beta, gamma, and high gamma bands (i.e., >16 Hz) are strongly correlated across recording sites. Statistically significant correlations are indicated by asterisks (*$P < 0.05$, bootstrap, FDR corrected). *C*: scatterplot of changes in mean response and intertrial variance of the low-frequency LFP (< 16 Hz) at each recording site during sustained stimulation. The correlation between these changes is not significantly different from zero ($R = 0.02$, $P = 0.33$, bootstrap). Each black dot shows the response from a recording site, and the gray ellipses show its variability. The horizontal/vertical diagonal of each ellipse shows the standard error of mean response and variance across the 30 stimuli. *D*: changes in total response power for each of the 309 recording sites. Data from each recording site are plotted as a short line, centered at the mean and spanning 1 standard error across the 30 stimuli on each site. The change in total power is near 0 dB for most recording sites, and 39% of recording sites show a decrease in total power.

intertrial variance, we then combined these frequency bands and examined their behavior across recording sites. Figure 3, *C* and *D*, show that stimulus-related changes in both intertrial variance and mean response of low-frequency LFP (<16 Hz) are highly variable across recording sites but the correlation between these two changes is not significantly different from zero (Fig. 3*C*; $R = 0.02$, $P = 0.33$). Since the mean response can be affected by the number of stimulus repetitions (see METHODS), we also considered the subset of sites for which each stimulus was repeated the same number of times (i.e., 5 repetitions, $N = 259$). Within this subset of recordings, the correlation between stimulus-related changes in mean response and variance remains low and not significantly different from zero ($P = 0.005$, $R = 0.48$).

The average stimulus-related change in total power is close to 0 (Fig. 3*D*). Therefore, for low-frequency LFP, the response averaged over recording sites is consistent with the phase resetting model (Fig. 1*A*). However, the behavior of individual recording sites varies widely, and the responses at any individual site might be consistent with any of the six cases illustrated in Fig. 1.

Spectro-temporal tuning of changes in LFP response variance. In the analyses above, neural activity was averaged across stimuli to characterize the average LFP response to many different speech stimuli. However, it has been shown, with linear STRF analysis, that mean LFP response is tuned to specific sound features (Eggermont et al. 2011). We used STRF analysis to test whether the intertrial variance of the LFP is also tuned to spectro-temporal stimulus features. We compared the tuning of the LFP variance with the tuning of MUA and the mean LFP response at the same recording site.

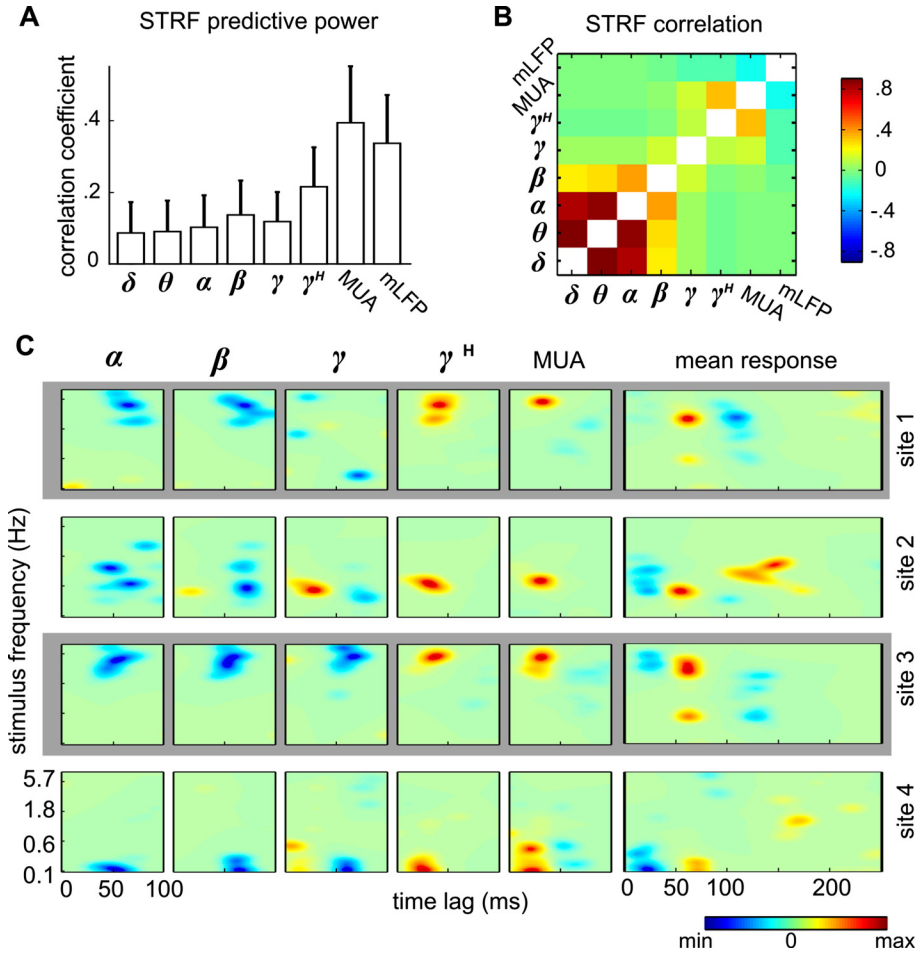

Fig. 4. LFP variance-based and MUA-based STRFs. *A*: the average prediction correlation, which indicates how well an STRF predicts the time-varying neural response, is higher for MUA and mean LFP (mLFP) response. The MUA is defined as the total power of the neural recording between 600 and 3,000 Hz. The LFP variance-based STRFs are used to model the intertrial variance of the LFP. *B*: correlation between the shape of STRFs measures the similarity of tuning across neural signals. Delta-, theta-, and alpha-variance STRFs are highly correlated, and the higher frequency bands (gamma, high gamma, MUA) also show a cluster of similarity to each other. *C*: example STRFs in each row are measured for the same recording site but using different LFP bands. Red areas indicate an increase in the neurophysiological signal following an increase in power of the corresponding spectro-temporal stimulus feature, and blue areas indicate a decrease. STRFs are normalized to have the same maximum absolute value. LFP variance STRFs are generally inhibitory in the alpha and beta bands, variable (inhibitory or excitatory) in the gamma band, and excitatory in the high gamma band. MUA STRFs are generally excitatory. The peak latency of the LFP variance STRF is later in the alpha and beta bands than in the high gamma band. The frequency tuning of LFP variance STRFs is generally similar to that of the MUA STRF but usually has additional peaks. Unlike the other signals, STRFs for mean LFP show peaks at multiple latencies. These STRFs typically show an early peak (~25 ms latency) with negative polarity indicating depolarization, followed by a positive peak (~60 ms latency) indicating hyperpolarization, and sometimes other longer-latency peaks.

Variance STRFs were estimated separately for each LFP frequency band. Significant sensory tuning was tested by measuring the ability of STRFs to predict the time-varying LFP signal, using a cross-validation procedure (Fig. 4*A*). Prediction performance was quantified by the correlation coefficient (Pearson's r) between the predicted and actual LFP. Average predictive power was significantly greater than chance in all bands [$P < 10^{-10}$, paired t-test, false discovery rate (FDR)-corrected for multiple comparisons] (Benjamini and Hochberg 1995). Although average predictive power was significantly different between all pairs of frequency bands ($P < 0.05$, paired t-test, FDR corrected), performance for the LFP variance bands was lower than for MUA and the mean LFP response.

The similarity of STRF tuning for different frequency bands is shown in Fig. 4*B*. Each point in the correlation matrix indicates the average correlation between STRFs estimated from two different neural signals. Variance STRFs are highly correlated between the delta, theta, and alpha bands ($R > 0.8$) and less correlated between other bands ($R < 0.4$). Because of the strong correlation between the delta-, theta-, and alpha-variance STRFs, in the following we report results only for the alpha band. Results for the delta and theta bands were nearly identical.

Figure 4*C* shows example STRFs from four recording site exemplars. In the alpha and beta bands, variance STRFs are consistently inhibitory, indicating a decrease in variance following increased power of the relevant spectro-temporal stimulus feature. The high-gamma variance STRF and MUA STRF are generally excitatory, indicating an increase in activity following increased power of the relevant stimulus feature. For the gamma band, variance STRFs are sometimes excitatory and sometimes inhibitory, suggesting that the gamma band spans a transition zone between distinct processes captured separately in low and high frequencies (see also Crone et al. 2001). The STRF estimated with the mean LFP response is more complex than the other signals, showing multiple peaks with alternating polarities. Because the mean response is the LFP waveform averaged over trials rather than a power or variance measure, its polarity does not indicate excitation or inhibition but rather net depolarization or hyperpolarization at the recording site.

The temporal properties of the neural response were characterized by summing each STRF across the frequency axis. The resulting one-dimensional function of time, called the temporal response function, averaged across all 477 recording sites, is shown for the different LFP bands in Fig. 5*A*. The MUA and high-gamma variance temporal response function shows positive peaks at relatively short latencies around 20–30 ms, indicating a rapid increase in high-gamma variance following favorable stimulus features. The alpha and beta variance temporal response function shows negative peaks at longer latencies around 40–50 ms, indicating a slower decrease in alpha/beta variance following favorable stimulus features. The gamma-band variance temporal response function shows an early positive peak (latency around 20 ms) followed by a

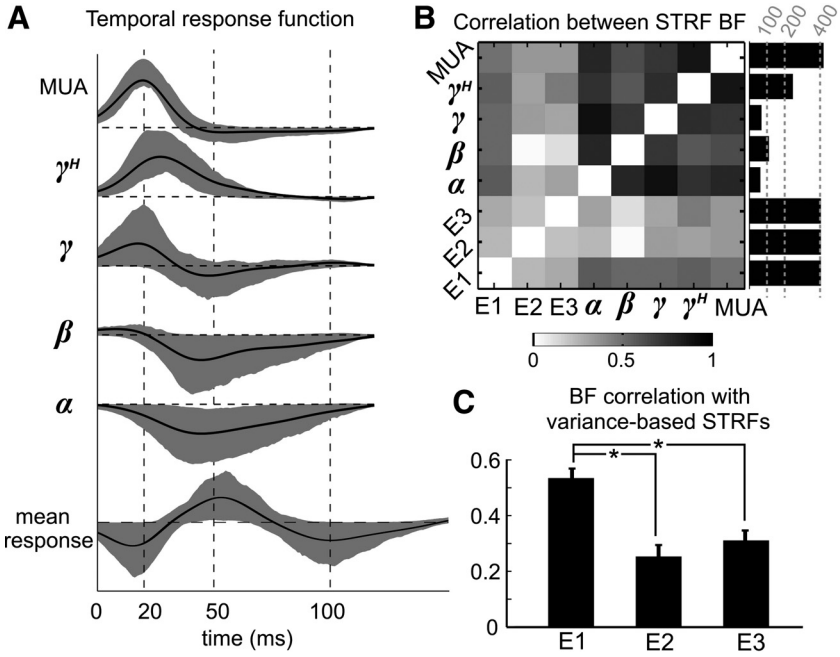

Fig. 5. Spectral and temporal properties of band-dependent STRFs. *A*: the average temporal response function (peak-normalized for each site) is plotted for each MUA and LFP band. Shading indicates the range between the 25th and 75th percentiles across sites. Vertical dashed lines mark peak response latencies for the mean LFP for comparison with the other traces. *B*: correlations between BF measured from STRFs for the different signals. BF is consistently similar between LFP variance STRFs and MUA STRFs, indicating similar frequency tuning. The 3 peaks in the STRF for mean LFP are analyzed separately, labeled E1, E2, and E3, with increasing latency. BFs of the 3 peaks are not strongly correlated with each other, but BF of the first peak is more correlated with that of MUA and LFP variance STRFs. The correlation between all pairs of measures is statistically significant ($P < 0.05$, bootstrap, FDR corrected), except that the BF of beta variance is not significantly correlated with the BFs of E1 and E2. Bar graph on *right* shows the number of recording sites included for each band in this analysis (i.e., sites with predictive power > 0.2). *C*: average correlation between the BF of each peak in the mean LFP and the BF of variance STRFs. The correlation coefficient is averaged across variance STRFs for all frequency bands (*$P < 0.05$, FDR corrected).

negative peak (latency around 50 ms), reflecting an initial increase in gamma-band variance followed by a decrease. As suggested by the full STRF analysis above (Fig. 4*C*), the temporal response function for the mean LFP response is more complicated, showing three peaks with alternating polarities at a group level. A positive peak in the LFP STRF indicates voltage changes toward hyperpolarization, while a negative peak indicates changes toward depolarization. Individual recording sites usually show more than one peak but not necessarily all the three peaks (Fig. 4*C*).

The similarity of frequency tuning between STRFs for different neural signals is characterized in Fig. 5*B*. Only STRFs with predictive power $r > 0.2$ were included in this analysis, and the number of recording site pairs involved in the correlation analysis is shown in Fig. 5*B*, *right*. BF is highly correlated for LFP variance and MUA, indicating that spectral tuning is similar in all the LFP variance bands as well as MUA. The three peaks in the mean-LFP STRF are analyzed separately. The BFs of the three peaks are not strongly correlated with each other, but the BF of the first peak shows a greater correlation across sites with the BF of other bands, compared with the second and third peaks (Fig. 5*C*).

DISCUSSION

By analyzing extracellular recordings from A1 of awake ferrets, we found that continuous natural sound affects not only the mean LFP response but also the variability of the LFP signal across trials. These stimulus-related changes in variability differ across LFP frequency bands. Auditory stimuli suppress the intertrial variance of low-frequency LFP (<16 Hz) but increase the intertrial variance in the high gamma band. Dynamic fluctuations in LFP variance are tuned to spectro-temporal acoustic features, and the auditory tuning of these fluctuations is correlated with the frequency tuning of MUA at the same recording site.

Sound reduces variance of low-frequency LFP. When stimulus-related effects are averaged across A1, a stimulus reduces the intertrial variance of low-frequency LFP (<16 Hz) and enhances the mean response. Similar phenomena have also been observed in humans with electrocorticography and MEG (Edwards et al. 2009; Fujioka et al. 2012; Howard and Poeppel 2012). The simultaneous increase in mean and decrease in variance enhance the precision of neural phase locking. Furthermore, these balanced changes lead to a net change of near zero in the total LFP power, consistent with the idea that global homeostatic processes maintain a relatively constant level of activity in cortex (Churchland et al. 2010; Fiser et al. 2004).

Although complementary on average, the relative size of changes in the mean response and response variance differs widely across recording sites, suggesting separable mechanisms controlling the changes in mean response and variance. Moreover, the changes in mean response and intertrial variance follow different time courses. The rise in the mean response is very rapid after stimulus onset (<50 ms), while the decrease in response variance is slower, taking ~300 ms. The slow dynamics of the variance decrease may be the reason why it is not reliably observed in transient responses to brief tones (Steinschneider et al. 2008) and becomes more evident as a dynamic sound sequence unfolds in time (Fuentemilla et al. 2006). One interpretation of this phenomenon is that changes in variance reflect processes by which the brain slowly adapts to the statistics of incoming sensory stimuli and encodes the stimulus more efficiently after reaching a steady state (Dean et al. 2005; Rabinowitz et al. 2011).

Additionally, our STRF measurements reveal that this suppression is often spectro-temporally tuned, in contrast to previous reports of feature-nonspecific reduction in variance (Churchland et al. 2010). This sensory tuning suggests that variance reduction is a phenomenon specific to local neural networks rather than a general, nonspecific process across A1.

Stimulus-related suppression of intertrial variance has been reported for both low-frequency LFP/EEG/MEG (Edwards et al. 2009; Fujioka et al. 2012; Howard and Poeppel 2012) and the firing rate of spiking activity (Buran et al. 2014; Church-

land et al. 2010). It is tempting to draw direct connections between these findings, but some caution should be taken when comparing LFP with single-unit spiking data. First, from a methodological perspective, low-frequency LFP is usually characterized by intertrial variability of the LFP waveform while the spiking activity is usually characterized by variability of the firing rate (rather than the highly variable spike time or the highly stereotyped and stable spike waveform). Spike rates can usually be modeled by a Poisson process, and for a Poisson process response variance is proportional to the mean response. In other words, the response variance always increases when the mean response increases. Instead, the variability of spiking activity is usually characterized by the Fano factor (i.e., the variance of the firing rate divided by the mean firing rate). A decreased Fano factor indicates a reduction in the rate by which the response variance increases relative to the mean. Second, a large component of the LFP reflects dendritic activity, comprising neural inputs in addition to output spikes. Thus the two signals may represent activity at different loci in the neural network (Carandini 2004). Third, changes in LFP mean and variance may be more tightly coupled to the synchrony of neural activity across populations rather than the variability of individual neural responses (Telenczuk et al. 2010). Thus changes in the reliability of a single neuron's spiking activity can have a complex relationship with the larger-scale LFP signal.

Implications for phase resetting models of low-frequency LFP oscillations. There are two dominant models for the interactions between stimulus-locked LFP responses and spontaneous neural oscillations. One, the phase resetting model, posits that some components of spontaneous neural oscillations are entrained to external stimuli and become the stimulus-locked responses (Hanslmayr et al. 2007; Kayser et al. 2009; Lakatos et al. 2009; Luo and Poeppel 2007; Makeig et al. 2002). The other model, referred to as the linear summation model, posits that stimulus-locked activity and spontaneous oscillations are independent and add linearly to produce measured neural signals (Ding and Simon 2013; Howard and Poeppel 2010, 2012; Makinen et al. 2005; Shah et al. 2004; Yeung et al. 2004). These two models both generate clear predictions about how the total LFP power and LFP variance should be affected by sensory input. The phase resetting model generally predicts that the total power of LFP is not changed by sensory stimuli and that the variance is reduced. The linear summation model, in contrast, predicts that the total LFP power is increased and the variance is not changed by the stimulus.

In contrast to either of these dominant models, this study finds that changes in mean response and variance are heterogeneous across local neural populations. Importantly, the total power of LFP is actually reduced at many recording sites, an effect that cannot be explained by either model or even by a combination of the two models. Therefore, suppression of spontaneous activity must be taken into consideration when modeling LFP responses (Buran et al. 2014). Furthermore, the present study did not reveal a significant correlation between the power of stimulus-locked activity and the reduction in intertrial variance, leaving it unclear as to whether stimulus-locked activity can be attributed exclusively to the phase resetting of spontaneous oscillations or to other neural mechanisms.

Sound enhances variance of high-frequency LFP. The natural sound stimulus produces a sustained increase in the intertrial variance of high-gamma-band LFP (~64–300 Hz) in A1. The time course of the high-gamma variance is similar to the time course of MUA (>600 Hz), which is strongly correlated with mean spike rate in the local area (Ray and Maunsell 2011). In the beta and alpha bands, changes in intertrial variance are more heterogeneous, with more recording sites showing a sustained decrease in the beta-band variance and a sustained increase in the gamma band. A similar dichotomy is also seen in the STRF analysis: The high-gamma STRF and MUA STRF are generally excitatory (Pasley et al. 2012), while the low-frequency (<16 Hz) LFP variance STRFs are generally inhibitory. Therefore, the stimulus-evoked behavior of LFP is qualitatively different between the low and high frequency bands. The low frequency bands (<16 Hz) show suppression, and the high frequency bands (>64 Hz) show enhancement. The transition between these two frequency regions lies in the beta and gamma range.

Mechanisms of intertrial response variability of neural activity. Why are the neural responses to the same stimulus variable across measurements? Two general explanations have been proposed. One explanation is that internal cortical state can strongly influence sensory processing. For example, in A1, spike timing is much more reliable in anesthetized animals compared with awake animals (Chaudhuri et al. 2015), and attention can further strongly modulate both spiking activity and LFP/EEG/MEG (Ding and Simon 2012a, 2012b; Fritz et al. 2003; Hasson et al. 2015; O'Sullivan et al. 2015; Woldorff and Hillyard 1991; Zion Golumbic et al. 2013). Recent studies also demonstrate that the trial-to-trial fluctuations of firing rate are correlated between neurons (Lin et al. 2015) and can be modeled by stimulus-independent fluctuations of cortical excitability (Ecker and Tolias 2014; Goris et al. 2014; Lin et al. 2015; McGinley et al. 2015). Our observation that changes in intertrial LFP variance are spectro-temporally tuned suggests that changes in LFP variance can be stimulus dependent. However, salient stimuli could also have bottom-up attention circuits (Kayser et al. 2005), leading to changes in behavioral state, which in turn influence variability through a more central mechanism.

A second possibility is that intrinsic activity in neural networks contributes to response variability. Intrinsic activity is ubiquitous in cortical circuits with or without any sensory stimulus. For the phase resetting theory (Fig. 1*A*), a component of intrinsic neural oscillations is phase reset by sensory stimuli while other components that are not phrase reset contribute to response variability (Hanslmayr et al. 2007; Kayser et al. 2009; Lakatos et al. 2009; Luo and Poeppel 2007; Makeig et al. 2002). For the additive response theory (Fig. 1, *B* and *C*), intrinsic neural activity is not affected by the stimulus, and such non-stimulus-locked activity contributes to response variability (Ding and Simon 2013; Howard and Poeppel 2010, 2012; Makinen et al. 2005; Shah et al. 2004; Yeung et al. 2004).

Conclusions. This study demonstrates that natural sound reduces the intertrial variance of low-frequency LFP below 16 Hz. The stimulus-related variance reduction is not correlated with the strength of the stimulus-locked LFP response, suggesting that separable neural mechanisms control the mean response and the response variance. This heterogeneity of the

relationship between mean response and variance may partly result from the differences between cortical layers, since phase resetting is often observed in the supragranular layers (Lakatos et al. 2005, 2008, 2009) and may be further strengthened in natural listening conditions because of the modulation of attention (Ding and Simon 2012a, 2012b; Fritz et al. 2003; Hasson et al. 2015; O'Sullivan et al. 2015; Woldorff and Hillyard 1991; Zion Golumbic et al. 2013) and stimulus modality (Lakatos et al. 2009).

Finally, the stimulus-related variance reduction is tuned to spectro-temporal features and the amount of reduction is highly variable across neural populations, suggesting that variance reduction is a property of local neural circuits rather than a global and homogeneous response across A1.

GRANTS

This work was supported by the National Institutes of Health (R00 DC-010439 to S. V. David, R01 DC-005779 to S. A. Shamma, R01 DC-008342 to J. Z. Simon), the Fundamental Research Funds for the Central Universities (N. Ding), Zhejiang Provincial Natural Science Foundation of China (LR16C090002 to N. Ding), and the European Research Council (ERC 295603 to S. A. Shamma).

DISCLOSURES

No conflicts of interest, financial or otherwise, are declared by the author(s).

AUTHOR CONTRIBUTIONS

Author contributions: N.D. and S.V.D. conception and design of research; N.D. analyzed data; N.D., J.Z.S., S.A.S., and S.V.D. interpreted results of experiments; N.D. prepared figures; N.D. and S.V.D. drafted manuscript; N.D., J.Z.S., S.A.S., and S.V.D. edited and revised manuscript; N.D., J.Z.S., S.A.S., and S.V.D. approved final version of manuscript; S.V.D. performed experiments.

REFERENCES

Benjamini Y, Hochberg Y. Controlling the false discovery rate: a practical and powerful approach to multiple testing. *J R Stat Soc Ser B* 57: 289–300, 1995.

Buran BN, von Trapp G, Sanes DH. Behaviorally gated reduction of spontaneous discharge can improve detection thresholds in auditory cortex. *J Neurosci* 34: 4076–4081, 2014.

Carandini M. Amplification of trial-to-trial response variability by neurons in visual cortex. *PLoS Biol* 2: 1483–1493, 2004.

Chaudhuri R, Knoblauch K, Gariel MA, Kennedy H, Wang XJ. A large-scale circuit mechanism for hierarchical dynamical processing in the primate cortex. *Neuron* 88: 419–431, 2015.

Churchland MM, Yu BM, Cunningham JP, Sugrue LP, Cohen MR, Corrado GS, Newsome WT, Clark AM, Hosseini P, Scott BB, Bradley DC, Smith MA, Kohn A, Movshon JA, Armstrong KM, Moore T, Chang SW, Snyder LH, Lisberger SG, Priebe NJ, Finn IM, Ferster D, Ryu SI, Santhanam G, Sahani M, Shenoy KV. Stimulus onset quenches neural variability: a widespread cortical phenomenon. *Nat Neurosci* 13: 369–378, 2010.

Crone NE, Boatman D, Gordon B, Hao L. Induced electrocorticographic gamma activity during auditory perception. *Clin Neurophysiol* 112: 565–582, 2001.

David SV, Mesgarani N, Fritz JB, Shamma SA. Rapid synaptic depression explains nonlinear modulation of spectro-temporal tuning in primary auditory cortex by natural stimuli. *J Neurosci* 29: 3374–3386, 2009.

David SV, Mesgarani N, Shamma SA. Estimating sparse spectro-temporal receptive fields with natural stimuli. *Network* 18: 191–212, 2007.

Dean I, Harper NS, McAlpine D. Neural population coding of sound level adapts to stimulus statistics. *J Neurosci* 8: 1684–1689, 2005.

Ding N, Simon JZ. Emergence of neural encoding of auditory objects while listening to competing speakers. *Proc Natl Acad Sci USA* 109: 11854–11859, 2012a.

Ding N, Simon JZ. Neural coding of continuous speech in auditory cortex during monaural and dichotic listening. *J Neurophysiol* 107: 78–89, 2012b.

Ding N, Simon JZ. Power and phase properties of oscillatory neural responses in the presence of background activity. *J Comput Neurosci* 34: 337–343, 2013.

Ecker AS, Tolias AS. Is there signal in the noise? *Nat Neurosci* 17: 750–751, 2014.

Edwards E, Soltani M, Kim W, Dalal SS, Nagarajan SS, Berger MS, Knight RT. Comparison of time-frequency responses and the event-related potential to auditory speech stimuli in human cortex. *J Neurophysiol* 102: 377–386, 2009.

Eggermont J, Munguia R, Pienkowski M, Shaw G. Comparison of LFP-based and spike-based spectro-temporal receptive fields and cross-correlation in cat primary auditory cortex. *PLoS One* 6: e20046, 2011.

Eggermont JJ. Temporal modulation transfer functions in cat primary auditory cortex: separating stimulus effects from neural mechanisms. *J Neurophysiol* 87: 305–321, 2002.

Fiser J, Chiu C, Weliky M. Small modulation of ongoing cortical dynamics by sensory input during natural vision. *Nature* 431: 573–578, 2004.

Fritz J, Shamma S, Elhilali M, Klein D. Rapid task-related plasticity of spectrotemporal receptive fields in primary auditory cortex. *Nat Neurosci* 6: 1216–1223, 2003.

Fuentemilla LI, Marco-Pallarés J, Grau C. Modulation of spectral power and of phase resetting of EEG contributes differentially to the generation of auditory event-related potentials. *Neuroimage* 30: 909–916, 2006.

Fujioka T, Trainor LJ, Large EW, Ross B. Internalized timing of isochronous sounds is represented in neuromagnetic beta oscillations. *J Neurosci* 32: 1791–1802, 2012.

Garofolo JS. *TIMIT: Acoustic-Phonetic Continuous Speech Corpus*. Philadelphia, PA: Linguistic Data Consortium, 1993.

Goris RL, Movshon JA, Simoncelli EP. Partitioning neuronal variability. *Nat Neurosci* 17: 858–865, 2014.

Hackett TA. Information flow in the auditory cortical network. *Hear Res* 271: 133–146, 2011.

Hanslmayr S, Klimesch W, Sauseng P, Gruber W, Doppelmayr M, Freunberger R, Pecherstorfer T, Birbaumer N. Alpha phase reset contributes to the generation of ERPs. *Cereb Cortex* 17: 1–8, 2007.

Hasson U, Chen J, Honey CJ. Hierarchical process memory: memory as an integral component of information processing. *Trends Cogn Sci* 19: 304–313, 2015.

Howard MF, Poeppel D. Discrimination of speech stimuli based on neuronal response phase patterns depends on acoustics but not comprehension. *J Neurophysiol* 104: 2500–2511, 2010.

Howard MF, Poeppel D. The neuromagnetic response to spoken sentences: co-modulation of theta band amplitude and phase. *Neuroimage* 60: 2118–2127, 2012.

Kayser C, Montemurro MA, Logothetis NK, Panzeri S. Spike-phase coding boosts and stabilizes information carried by spatial and temporal spike patterns. *Neuron* 61: 597–608, 2009.

Kayser C, Petkov CI, Lippert M, Logothetis NK. Mechanisms for allocating auditory attention: an auditory saliency map. *Curr Biol* 15: 1943–1947, 2005.

Krause BM, Banks MI. Analysis of stimulus-related activity in rat auditory cortex using complex spectral coefficients. *J Neurophysiol* 110: 621–639, 2013.

Lakatos P, Karmos G, Mehta AD, Ulbert I, Schroeder CE. Entrainment of neuronal oscillations as a mechanism of attentional selection. *Science* 320: 110–113, 2008.

Lakatos P, O'Connell MN, Barczak A, Mills A, Javitt DC, Schroeder CE. The leading sense: supramodal control of neurophysiological context by attention. *Neuron* 64: 419–430, 2009.

Lakatos P, Shah AS, Knuth KH, Ulbert I, Karmos G, Schroeder CE. An oscillatory hierarchy controlling neuronal excitability and stimulus processing in the auditory cortex. *J Neurophysiol* 94: 1904–1911, 2005.

Lewicki MS. Efficient coding of natural sounds. *Nat Neurosci* 5: 356–363, 2002.

Lin IC, Okun M, Carandini M, Harris KD. The nature of shared cortical variability. *Neuron* 87: 644–656, 2015.

Luo H, Poeppel D. Phase patterns of neuronal responses reliably discriminate speech in human auditory cortex. *Neuron* 54: 1001–1010, 2007.

Makeig S, Westerfield M, Jung TP, Enghoff S, Townsend J, Courchesne E, Sejnowski TJ. Dynamic brain sources of visual evoked responses. *Science* 295: 690–694, 2002.

Makinen V, Tiitinen H, May P. Auditory event-related responses are generated independently of ongoing brain activity. *Neuroimage* 24: 961–968, 2005.

McGinley MJ, David SV, McCormick DA. Cortical membrane potential signature of optimal states for sensory signal detection. *Neuron* 87: 179–192, 2015.

O'Sullivan JA, Power AJ, Mesgarani N, Rajaram S, Foxe JJ, Shinn-Cunningham BG, Slaney M, Shamma SA, Lalor EC. Attentional selection in a cocktail party environment can be decoded from single-trial EEG. *Cereb Cortex* 25: 1697–1706, 2015.

Pasley BN, David SV, Mesgarani N, Flinker A, Shamma SA, Crone NE, Knight RT, Chang EF. Reconstructing speech from human auditory cortex. *PLoS Biol* 10: e1001251, 2012.

Rabinowitz NC, Willmore BD, Schnupp JW, King AJ. Contrast gain control in auditory cortex. *Neuron* 70: 1178–1191, 2011.

Ray S, Maunsell JH. Different origins of gamma rhythm and high-gamma activity in macaque visual cortex. *PLoS Biol* 9: e1000610, 2011.

Shah AS, Bressler SL, Knuth KH, Ding M, Mehta AD, Ulbert I, Schroeder CE. Neural dynamics and the fundamental mechanisms of event-related brain potentials. *Cereb Cortex* 14: 476–483, 2004.

Singh NC, Theunissen FE. Modulation spectra of natural sounds and ethological theories of auditory processing. *J Acoust Soc Am* 114: 3394–3411, 2003.

Steinschneider M, Fishman YI, Arezzo JC. Spectrotemporal analysis of evoked and induced electroencephalographic responses in primary auditory cortex (A1) of the awake monkey. *Cereb Cortex* 18: 610–625, 2008.

Szymanski FD, Rabinowitz NC, Magri C, Panzeri S, Schnupp JW. The laminar and temporal structure of stimulus information in the phase of field potentials of auditory cortex. *J Neurosci* 31: 15787–15801, 2011.

Tallon-Baudry C, Bertrand O. Oscillatory gamma activity in humans and its role in object representation. *Trends Cogn Sci* 3: 151–162, 1999.

Telenczuk B, Nikulin VV, Curio G. Role of neuronal synchrony in the generation of evoked EEG/MEG responses. *J Neurophysiol* 104: 3557–3567, 2010.

Truccolo WA, Ding M, Knuth KH, Nakamura R, Bressler SL. Trial-to-trial variability of cortical evoked responses: implications for the analysis of functional connectivity. *Clin Neurophysiol* 113: 206–226, 2002.

Woldorff MG, Hillyard SA. Modulation of early auditory processing during selective listening to rapidly presented tones. *Electroencephalogr Clin Neurophysiol* 79: 170–191, 1991.

Yeung N, Bogacz R, Holroyd CB, Cohen JD. Detection of synchronized oscillations in the electroencephalogram: an evaluation of methods. *Psychophysiology* 41: 822–832, 2004.

Zion Golumbic EM, Ding N, Bickel S, Lakatos P, Schevon CA, McKhann GM, Goodman RR, Emerson R, Mehta AD, Simon JZ, Poeppel D, Schroeder CE. Mechanisms underlying selective neuronal tracking of attended speech at a "cocktail party." *Neuron* 77: 980–991, 2013.